JSSS
Journal of Sensors
and Sensor Systems

Cyclic and square-wave voltammetry for selective simultaneous NO and O$_2$ gas detection by means of solid electrolyte sensors

Anastasiya Ruchets[1], Nils Donker[2], Jens Zosel[1], Daniela Schönauer-Kamin[2], Ralf Moos[2], Ulrich Guth[3], and Michael Mertig[1,3]

[1]Kurt-Schwabe-Institut für Mess- und Sensortechnik Meinsberg e.V., Kurt-Schwabe-Straße 4, 04736 Waldheim, Germany
[2]Department of Functional Materials, University of Bayreuth, Universitätsstraße 30, 95440 Bayreuth, Germany
[3]Institute of Physical Chemistry, Technische Universität Dresden, 01062 Dresden, Germany

Correspondence: Anastasiya Ruchets (anastasiya.ruchets@ksi-meinsberg.de)

Abstract. Solid electrolyte gas sensors (SESs) based on yttria-stabilized zirconia (YSZ) are suitable to detect traces of redox components in inert gases. Usually, their signals are generated as a voltage between two electrodes at open circuit potential or as a current flowing between constantly polarized electrodes. In these rather stationary modes of operation, SESs often lack the desired selectivity. This drawback can be circumvented if SESs are operated in dynamic electrochemical modes that utilize the differences of electrode kinetics for single components to distinguish between them. Accordingly, this contribution is directed to the investigation of cyclic voltammetry and square-wave voltammetry as methods to improve the selectivity of SESs. For this, a commercial SES of the type "sample gas, Pt|YSZ|Pt, air" was exposed to mixtures containing NO and O$_2$ in N$_2$ in the temperature range between 550 and 750 °C.

On cyclic voltammograms (CVs), NO-related peaks occur in the cathodic direction at polarization voltages between -0.3 and -0.6 V at scan rates between 100 and 2000 mV s^{-1} and temperatures between 550 and 750 °C. Their heights depend on the NO concentration, on the temperature and on the scan rate, providing a lower limit of detection below 10 ppmv, with the highest sensitivity at 700 °C. The O$_2$-related peaks, appearing also in the cathodic direction between -0.1 and -0.3 V at scan rates between 100 and 5000 mV s^{-1}, are well separated from the NO-related peaks if the scan rate does not exceed 2000 mV s^{-1}.

Square-wave voltammograms (SWVs) obtained at a pulse frequency of 5 Hz, pulses of 0.1 mV and steps of 5 mV in the polarization range from 0 to -0.6 V also exhibit NO-related peaks at polarization voltages between -0.3 and -0.45 V compared to the Pt–air (platinum–air) electrode. In the temperature range between 650 and 750 °C the highest NO sensitivity was found at 700 °C. O$_2$-related peaks arise in the cathodic direction between -0.12 and -0.16 V, increase with temperature and do not depend on the concentration of NO. Since capacitive currents are suppressed with square-wave voltammetry, this method provides improved selectivity. In contrast to cyclic voltammetry, a third peak was found with square-wave voltammetry at -0.48 V and a temperature of 750 °C. This peak does not depend on the NO concentration. It is assumed that this peak is due to the depletion of an oxide layer on the electrode surface. The results prove the selective detection of NO and O$_2$ with SESs operated with both cyclic voltammetry and square-wave voltammetry.

1 Introduction

To detect traces of redox active components beside oxygen in inert gases such as Ar, N_2 and He, ZrO_2-based solid electrolyte sensors (SESs) can be used. The solid electrolyte with considerable oxide ions' conductivity at temperatures above $500\,°C$ is thermodynamically highly stable and can be operated with various static (potentiometry, amperometry; Möbius, 1991) or dynamic methods (pulsed polarization; Fischer et al., 2014; cyclic voltammetry; Schelter et al., 2016). In static mode, the selectivity of such sensors is limited, so that it is usually not possible to distinguish between individual gas components. In contrast, dynamic methods allow a significantly increased selectivity by using different rates of the electrode reactions of the individual components in order to detect them independently (Teske et al., 1986; Yi et al., 1993; Shoemaker, 1996; Miura et al., 1998; Schelter et al., 2013; Fischer et al., 2014; Schelter et al., 2016; Ritter et al., 2018).

It has been shown previously that for simultaneous measurement of O_2 and CO such methods as cyclic voltammetry can be used (Zhang et al., 2017), while NO/NO_2 in O_2-containing N_2 could be detected by pulsed polarization (Donker et al., 2019). Furthermore, H_2, O_2 and H_2O were selectively detected in N_2 by means of cyclic voltammetry with the commercial SES used in this work (Ruchets et al., 2019). Square-wave voltammetry was also applied to H_2, O_2 and CO detection but showed ambivalent results (Schelter, 2015).

In this work the abilities of cyclic voltammetry and square-wave voltammetry for selective and comprehensive multiple gas detection were investigated using the example of NO and O_2, also to elucidate probable electrode reaction mechanisms.

2 Experiment

The test setup shown in Fig. 1 is described in detail elsewhere (Ruchets et al., 2019). It consists of two sequentially connected SESs manufactured by Zirox Sensoren & Elektronik GmbH, Greifswald, Germany. They were used to adjust the O_2 concentration (SES 1) and the electrochemical investigations in N_2 gas flow (SES 2), respectively. Mass flow controllers (MFCs) from Brooks Instrument Company, Hatfield, USA, were used for flow rate adjustment between 5 and 20 sccm (standard cubic centimetres per minute at $0\,°C$ and $101\,325\,Pa$). The N_2 base gas flow was purified by a triple filter for moisture, O_2 and hydrocarbon removal from Restek GmbH, Bad Homburg, Germany, to assure trace concentrations of these admixtures below 10 ppbv. For the electrochemical measurements a REF 600 potentiostat from Gamry Instruments, Warminster, USA, was used. All gas supply lines have been equipped with stainless steel tubes and screwed connectors from Swagelok, Solon, OH, USA.
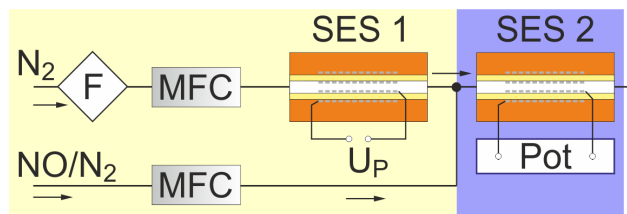
Figure 1. Experimental setup. MFC – mass flow controller, SES – solid electrolyte sensor, Pot – electrochemical measuring system, F – triple filter.

Both SESs of the type "sample gas, Pt|YSZ|Pt, air" contain an yttria-stabilized zirconia (YSZ) solid electrolyte tube with Pt electrodes on both sides and a porous YSZ sintered layer. The latter connects electrolyte and electrodes and covers large parts of the reference and measuring electrode. This provides an extended three-phase boundary for the rapid oxygen transfer. Both measuring and reference electrodes were made of Pt meshes with a length of 4 cm. The area of the measuring electrode was estimated from its dimensions and the mesh parameters to the value $3.5\,cm^2$.

SES 1 was continuously polarized at a constant voltage during each measurement, ensuring a constant O_2 concentration in the sample gas. Polarization voltage and O_2 concentration were varied between different types of measurements in the range $c(O_2) = 0.2$–450 ppmv. For SES 2, the voltammetric measurements were carried out at polarization voltages between -0.1 and -0.9 V for cyclic voltammetry and -0.1 and -0.6 V for square-wave voltammetry compared to the Pt–air (platinum–air) reference electrode. Cyclovoltammetric scan rates range between 100 and $5000\,mV\,s^{-1}$, while square-wave voltammograms (SWVs) were recorded at 5 Hz frequency, 5 mV steps and 0.1 mV pulses (see inset in Fig. 8). The second cycle of each CV was used to assess the results. Between two consecutive CVs as well as between SWVs, the cell voltage at open circuit potential (OCP) was measured to assure adequate cell depolarization.

3 Results and discussion

3.1 Cyclic voltammetry

The CVs shown in Fig. 2a display NO-related peaks arising in the cathodic direction between -0.2 and -0.7 V at scan rates between 100 and $2000\,mV\,s^{-1}$. The peak maximum shifts in the cathodic direction with increasing scan rate. The highest sensitivity of around $6.6\,\mu A\,ppmv^{-1}$ NO, i.e. the highest increase of the peak height with concentration, is achieved at $2000\,mV\,s^{-1}$. At higher scan rates the sensitivity decreases again, as shown on the CVs recorded at $5000\,mV\,s^{-1}$. The O_2-related peaks appear between -0.1 and -0.25 V and scan rates between 100 and $2000\,mV\,s^{-1}$. It was already shown in Ruchets et al. (2019) that the majority of O_2 reduced in these peaks is pumped into the cell when the
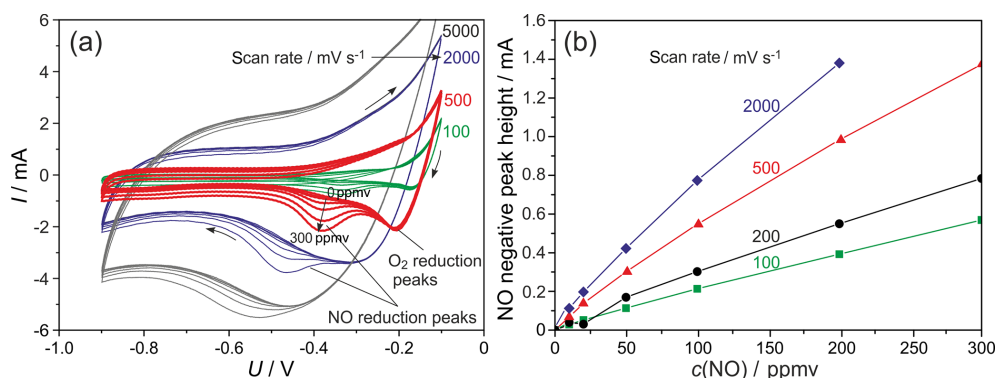
Figure 2. Cyclic voltammograms **(a)** and NO peak heights **(b)** at different potential scan rates and NO concentrations. Sensor temperature $T = 650\,^\circ\text{C}$; flow rate $= 10\,\text{sccm}$; $c(O_2) = 0.2\,\text{ppmv}$.

positive CV limit is passed. At a constant flow rate through the cell the fraction of pumped oxygen flowing out of the electrode section between the positive current maximum and the O_2 reduction peak decreases with increasing scan rate. Therefore, the opposite fraction of pumped O_2, which is reduced in the O_2 peak, increases with the scan rate.

With increasing scan rates, these O_2-related peaks are shifted in the cathodic direction and overlap the NO peaks progressively. At scan rates between 200 and 2000 mV s^{-1} the completely separated peaks of O_2 and NO allow us to distinguish between these gases and to measure NO selectively at concentrations above the lower limit of detection (approximately 10 ppmv). The horizontal curve shift that is visible at cathodic potentials below -0.55 V is nearly identical to the Faraday current calculable from the NO reduction. Higher scan rates also lead to a larger hysteresis between the currents in the cathodic and anodic direction at $U < -0.6$ V, which is attributed to be caused by the double-layer capacitance at the electrodes. The linear increase of capacitive current I_C (half of the hysteresis) with scan rate shown in the inset of Fig. 7 for a baseline CV was used to determine the double-layer capacitance as the ascend of the trend line $I_C / v_R = C_{DL} = 0.55$ mF. This very high capacitance may be due to the large area of the electrodes themselves as well as charge storage in the form of oxygen-containing species (Jaccoud et al., 2007).

The NO sensitivity of this method quantifies the increase of the signal (peak height) with the NO concentration. The peak height was determined as the maximum of the differences between the respective CV curve and the baseline at $c(NO) = 0$ ppmv at the same scan rate. These values are plotted in Fig. 2b as a function of the NO concentration for scan rates between 100 and 2000 mV s^{-1}. The sensitivity increases non-linearly with the scan rate up to 2000 mV s^{-1}, and its value at a fixed scan rate decreases slightly with rising NO concentration.

To characterize the possible reactions of NO at the measuring electrode, its open circuit potentials (OCPs) were also
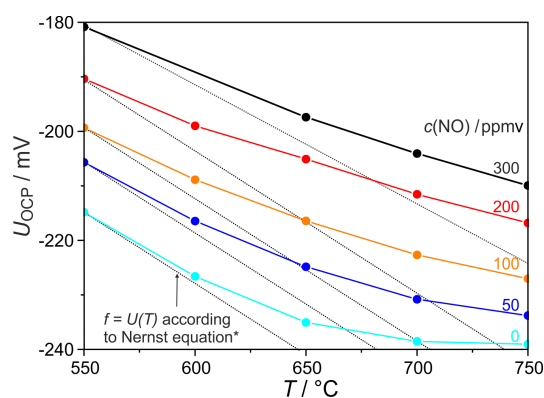

Figure 3. Dependence of the cell voltage at open circuit potential (U_{OCP}) on the sensor temperature T at different NO concentrations. Flow rate $= 10\,\text{sccm}$; $c(O_2) = 0.2\,\text{ppmv}$. * U_{OCP} curves at constant $p(O_2)$ in the sample gas at $T = 550\,^\circ\text{C}$.

measured as a function of temperature at different NO concentrations. The OCPs shown in Fig. 3 reflect the tendency of the nitrogen oxides to equilibrate at hot and catalytically active platinum electrodes according to Reactions (R1) and (R2):

$$2NO \rightleftharpoons O_2 + N_2 \qquad \text{(R1)}$$
$$2NO_2 \rightleftharpoons 2NO + O_2. \qquad \text{(R2)}$$

In the entire investigated temperature range the absolute value of the OCP decreases with increasing NO concentrations; i.e. according to the Nernst equation, the oxygen partial pressure $p(O_2)$ increases with the NO concentration. For comparison, the dashed lines in Fig. 3 show the voltage dependency that would result from the Nernst equation assuming a temperature-invariant $p(O_2)$. The measured OCP deviates from these theoretical values the more the temperature increases. This may be caused on the one hand by the temperature-dependent reaction equilibrium (Reaction R1). On the other hand, this rising deviation is related to an additional intake of O_2 into the sample gas through the YSZ
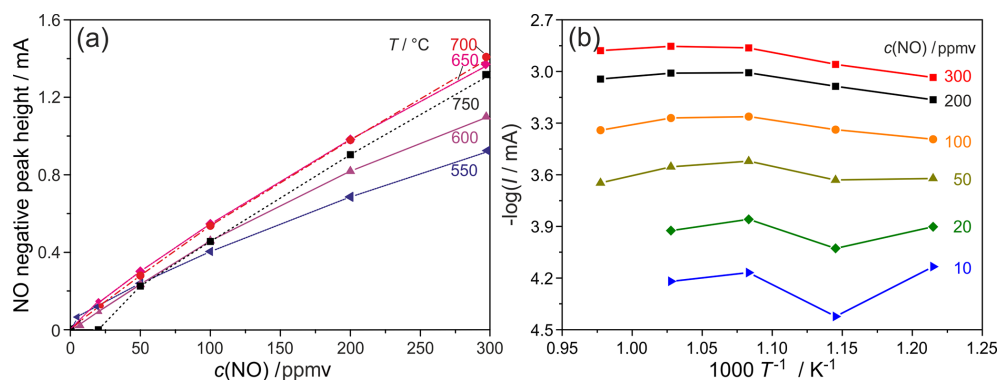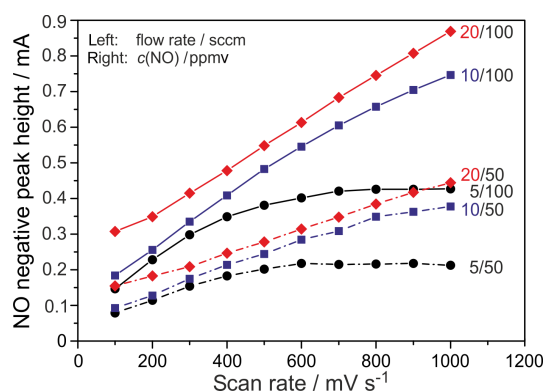
Figure 4. Dependence of NO peak heights on the NO concentration at different sensor temperatures **(a)** and Arrhenius dependency **(b)**. Flow rate $= 10$ sccm; $c(O_2) = 0.2$ ppmv.

electrolyte, carried by defect electron conductivity, which increases exponentially with temperature (Park and Blumenthal, 1989).

The comparison between the OCP values obtained at different NO concentrations and temperatures indicates that the OCP differences between two neighbouring concentrations are largest at temperatures in the range of 650–700 °C. These results thus provide an explanation for the NO peak formation in the CVs shown in Fig. 2 that is based on the reduction of the oxygen released from the NO decomposition according to Reaction (R1).

The NO peak heights also depend on temperature, as shown in Fig. 4a for a scan rate of $500\,\mathrm{mV\,s^{-1}}$. Here, the highest NO sensitivities were found at NO concentrations below 50 ppmv and temperatures between 650 and 750 °C. The sensitivity decreases with increasing NO concentration for all temperatures, as similarly found for the scan rate (see Fig. 2b). While this sensitivity decrease is very small in the range $T = 650$–$750\,°C$ and $c(NO) = 50$–300 ppmv, it becomes more pronounced at lower temperatures between 550 and 650 °C. It is assumed that the surface diffusion of NO as one of the most rate-limiting processes is mainly responsible for this sensitivity decrease at temperatures below 650 °C. The relatively small sensitivity changes at 650 °C and higher temperatures are presumed to be related to the interaction of diffusion and NO/NO_2 equilibrium at the measuring electrode, which is supported by the results in Fig. 3, where the $p(O_2)$ difference between the curves of 0 and 300 ppmv NO at the measuring electrode is significantly larger at 650 °C than at 550 and 750 °C.

In Fig. 5, the influence of the flow rate on the NO peak height is given at 750 °C sensor temperature and $c(O_2) = 10$ ppmv for the two NO concentrations, 50 and 100 ppmv. It was found that this parameter also influences the peak height considerably in the investigated range. The documented increase of the NO peak height with the flow rate indicates a limitation that appears more prominent the lower the flow rate and the higher the scan rate are. The curves


Figure 5. Dependence of the NO peak height on the scan rate at different flow rates and NO concentrations. $T = 750\,°C$; $c(O_2) = 10$ ppmv.

recorded at 5 sccm show a constant peak height at scan rates above $500\,\mathrm{mV\,s^{-1}}$ at 50 ppmv NO and above $700\,\mathrm{mV\,s^{-1}}$ at 100 ppmv NO. The curves at 10 sccm exhibit a slight bending, while the curves at 20 sccm show an almost linear increase at scan rates between 300 and $1000\,\mathrm{mV\,s^{-1}}$. This suggests that, in addition to the peak-forming limitation by surface diffusion at the platinum electrode, a further limitation by the analyte gas flow occurs, causing a combined influence of the peak height by the scan rate and volume flow.

If the peak height rises linearly with the square root of the scan rate at constant analyte concentration, the electrode reaction is completely diffusion-controlled, as described in the Randles–Ševčík equation (Randles, 1948; Ševčík, 1948). This behaviour was found for the NO peaks in this sensor only for the flow rate 20 sccm at scan rates between 500 and $2000\,\mathrm{mV\,s^{-1}}$ at all adjusted NO concentrations, as the curves in Fig. 6 prove. At lower sensor temperatures and flow rates, no Randles–Ševčík behaviour was found in the investigated range of scan rates. Furthermore, it could be shown that an O_2 concentration increase leads to a decrease of the NO peak. We assume that this shift is also caused by the shift of the
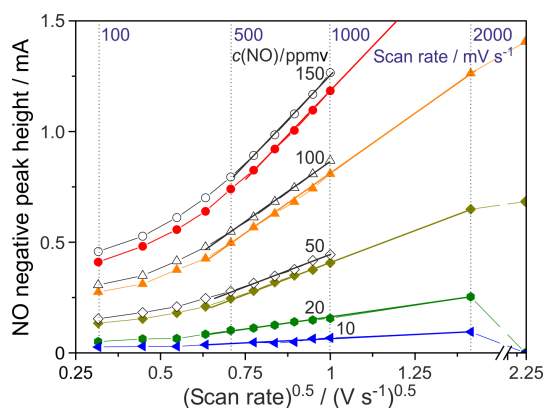
**Figure 6.** Dependence of the NO peak height on the square root of the scan rate. $T = 750\,^\circ C$; $c(O_2) = 0.2\,ppmv$ (black curves); $c(O_2) = 50\,ppmv$ (coloured curves).
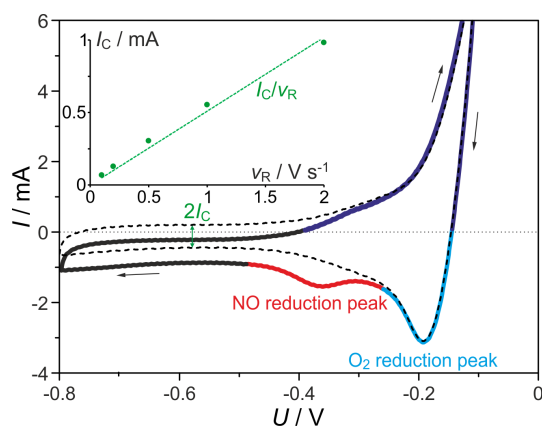
Figure 7. Typical CVs in NO containing gas and in pure N_2 (dashed line), O_2 pumping in current (dark blue line), O_2-related peak (light blue line), NO-related peak (red line). Inset: hysteresis dependency on the scan rate (v_r) for the baseline CVs in pure nitrogen gas flow for the double-layer capacitance calculation ($I_C/v_R = C_{DL}$). $c(NO) = 0\,ppmv$; $c(O_2) = 0.2\,ppmv$; flow rate $= 10\,sccm$; $T = 650\,^\circ C$.

equilibrium between NO, O_2 and NO_2 at the hot Pt electrode to lower NO concentrations with rising O_2 concentration (Crocoll and Weisweiler, 2004).

Summarizing a complete typical CV cycle as illustrated in Fig. 7, the following regions can be distinguished. Starting at $U = -0.1\,V$ in the cathodic direction (dark blue line), O_2 is pumped at an elevated rate into the sample gas flow and subsequently oxidizes NO to NO_2 partially. This O_2 input rapidly shrinks to zero when U reaches the OCP value. In this region the O_2 concentration at the sensor outlet is much higher than at the sensor inlet and is accompanied by a considerable amount of NO_2. During the following O_2 reduction peak between $U = -0.18$ and $-0.28\,V$ (light blue line), nearly all O_2 in the sample gas is pumped out, bringing the NO concentration back to its input value. Determination of the NO peak areas measured at different concentrations and
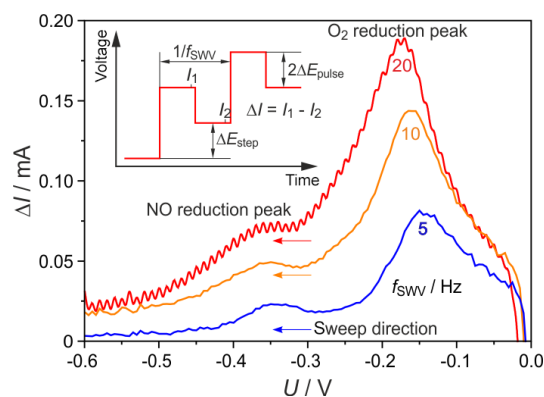
Figure 8. SWV at different frequencies (f_{SWV}); $\Delta E_{pulse} = 0.1\,mV$; $\Delta E_{step} = 5\,mV$; $c(NO) = 150\,ppmv$; $c(O_2) = 0.2\,ppmv$; flow rate $= 20\,sccm$; $T = 700\,^\circ C$.

Table 1. Comparison of signal-to-noise ratios (SNRs) of CV and SWV results given in Figs. 2a and 8.

| Method	v_R/mV s^{-1}; f_{SWV}/Hz	T/°C	$c(NO)$/ ppmv	SNR
CV	500	650	200	113
SWV	20	700	150	3
	10			13
	5			12

flow rates at $500\,mV\,s^{-1}$ indicates amounts of reduced NO ranging between 70 % and 90 % of the NO quantity passing the cell during peak development. Going further into cathodic polarization, all incoming NO and O_2 is reduced, until the point of zero current on the way back in the anodic direction (black curve). As already discussed, the differences between the currents measured in the cathodic and anodic direction at voltages $U < -0.6\,V$ are caused mainly by the double-layer capacitance C_{DL}. After crossing the zero current point in the anodic direction, O_2 is pumped into the measuring gas again (dark blue line). The small following peak does not depend on NO or O_2 concentration and is assumed to indicate the build-up of an electrode oxide layer.

3.2 Square-wave voltammetry

SWVs were conducted to figure out if omitting the influence of the capacitive charge helps to improve sensitivity and selectivity in comparison to cyclic voltammetry. As the curves in Fig. 8 illustrate, the difference between forward and backward current ΔI also exhibits peaks for O_2 and NO in similar potential ranges as for the CV measurements. At a temperature of $700\,^\circ C$, flow rate of $20\,sccm$, NO concentration of $150\,ppmv$ and O_2 concentration of $0.2\,ppmv$, the step frequency $5\,Hz$ (0.2 s step time) results in maximally separated NO and O_2 peaks with the highest peak resolution. Therefore, this $5\,Hz$ frequency was chosen for all following SWVs.
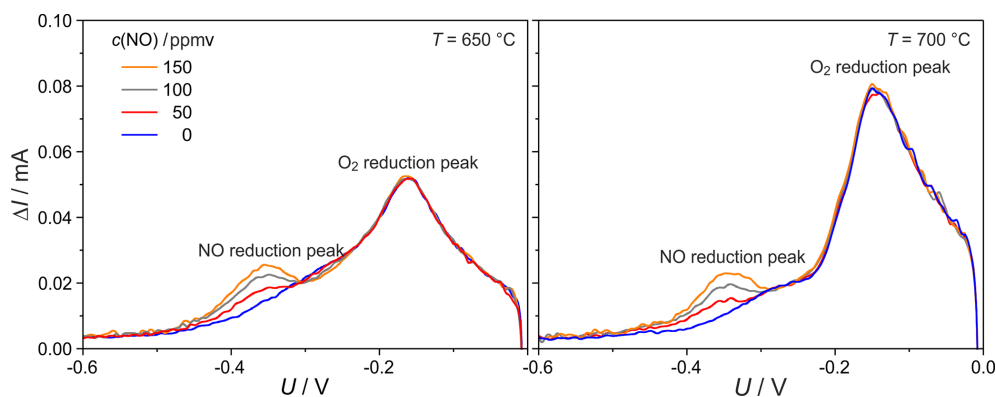
Figure 9. SWV at different temperatures and different NO concentrations. $f_{SWV} = 5\,Hz$; other experimental conditions as declared in Fig. 8.
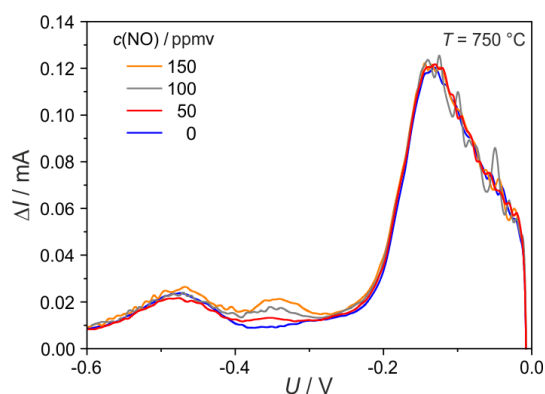
Figure 10. SWV at $T = 750\,°C$ and different NO concentrations; other experimental conditions as declared in Fig. 9.
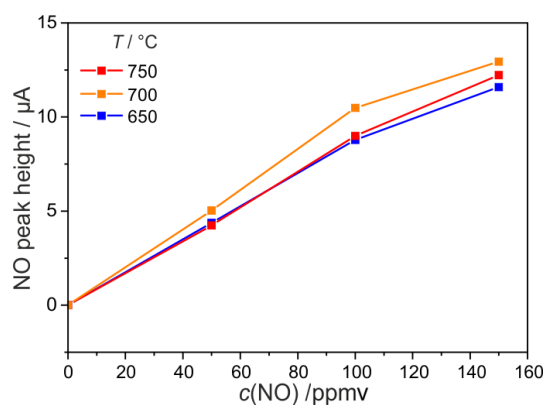
Figure 11. SWV peak height dependency on temperature and NO concentration dependency; other experimental conditions as declared in Fig. 9.

The O_2 peak maxima are shifted in the cathodic direction with increasing frequency. This increase causes faster potential sweep and is, therefore, analogous to the peak shift with increasing scan rate found in the CVs. A comparison between the NO-related peaks in Fig. 8 with two selected CV peaks illustrated in Fig. 2a for $500\,mV\,s^{-1}$ indicates a significantly lower signal-to-noise ratio of the SWV peaks. Values of this ratio were determined by dividing the peak height by the doubled standard deviation of the baseline current. As shown in Table 1, the signal-to-noise ratio of the SWV peaks decreases significantly at step frequencies above $10\,Hz$.

In Fig. 9, curves of ΔI for a flow rate of $20\,sccm$ and $c(O_2)$ of $0.2\,ppmv$ are given for different NO concentrations and temperatures. The NO-related peaks arise between -300 and $-450\,mV$. The peaks do not shift with NO concentration and are well separated from O_2-related peaks, thus providing highly selective multiple gas detection also with square-wave voltammetry. The sensitivity to NO amounts to nearly $0.1\,\mu A\,ppmv^{-1}$ NO at $650\,°C$.

Surprisingly, at $750\,°C$ a third peak arises in the SWV curves, with its maximum at $-480\,mV$ (see Fig. 10), which could not be detected previously in all measured CVs. This

peak does not depend on the NO concentration but (as it is shown later) on the O_2 concentration. Therefore, it is assumed that this peak is caused by an electrode process that removes oxygen from the electrode–electrolyte interface. It appears at low O_2 concentrations in the flow and temperature higher than $700\,°C$.

Calculating the SWV peak height in the same way as described for the CV peaks, its temperature dependence was determined in the range from 650 to $750\,°C$ as shown in Fig. 11. Between 10 and $100\,ppmv$, the NO peak increases linearly with the NO concentration. At higher concentrations, the sensitivity decreases. As described already for the temperature influence on the NO peak height in the CV between 650 and $750\,°C$, the SWV peaks related to NO also reach their maximum height at $700\,°C$ and are slightly lower at 650 and $750\,°C$. In contrast to that, the O_2-related peak in the range from -135 to $-160\,mV$ depends strongly on temperature, since the amount of pumped O_2 increases with the electrolyte conductivity. It is interesting to note that with square-wave voltammetry, an NO sensitivity was found at scan rates that would not provide any sensitivity with cyclic voltamme-
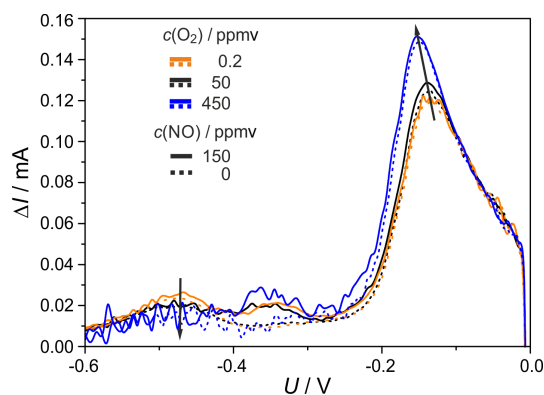
Figure 12. SWV at different O_2 concentrations and $T = 750\,°C$; other experimental conditions as declared in Fig. 9.

try (SWV at 5 Hz and 5 mV step height corresponds to cyclic voltammetry at $25\,mV\,s^{-1}$).

The influence of the O_2 concentration on the heights of the detected peaks is shown in Fig. 12, with curves at 0.2, 50 and 450 ppmv O_2 and 0 and 150 ppmv NO. Since forward and backward currents are an order of magnitude higher at 450 ppmv O_2 than at 50 ppmv O_2, their difference ΔI is much noisier at the high O_2 concentration. The O_2 peak increases as expected with the O_2 concentration. The NO-related peak shows nearly no dependence on the O_2 concentration. The peak associated with the oxygen-removing electrode process decreases with the O_2 concentration. This supports the assumption of oxygen removal from the electrode–electrolyte interface.

4 Summary

A commercial solid electrolyte sensor based on yttria-stabilized zirconia was operated in flow mode by means of cyclic voltammetry and square-wave voltammetry. It has been shown that beside O_2, NO can also be detected selectively and independently under certain conditions using both dynamic techniques.

The heights of the measured CV peaks increase non-linearly with the NO concentration in the range from 0 to 300 ppmv between 550 and 750 °C. The NO detection limit is lower than 10 ppmv. With square-wave voltammetry, NO peaks were also detected. They are well separated from the O_2 peaks. The NO peak height depends linearly on the NO concentration between 10 and 100 ppmv between 650 and 750 °C, while between 100 and 150 ppmv, the sensitivity decreases. Applying cyclic voltammetry, NO peaks occur at polarization voltages between −0.3 and −0.6 V, while applying square-wave voltammetry, NO peaks increase between −0.3 and −0.45 V compared to the Pt/air electrode. The O_2 reduction peaks were found at polarization voltages between −0.1 and −0.3 V with cyclic voltammetry and between −0.12 and −0.16 V with square-wave voltammetry. The highest

NO sensitivity was found at 700 °C for both dynamic methods. As one possible reason for this sensitivity maximum, an oxygen exchange process is assumed starting above 700 °C and resulting in an additional peak in the SWVs. The peak-forming diffusion limitation occurs in the gas flow as well as on the electrode surface so that the peak height increases with the scan rate as well as with the flow rate up to 20 sccm. Sensitivity and selectivity of both methods do not differ at larger scale. Maximum values of sensitivities amount to 6.6 and $0.1\,\mu A\,ppmv^{-1}$ NO for cyclic voltammetry and square-wave voltammetry, respectively. The advantage of omitting capacitive currents with square-wave voltammetry is gained by a reduced signal-to-noise ratio of this method. The results prove the selective detection of NO and O_2 with SESs operated with both cyclic voltammetry and square-wave voltammetry.

Author contributions. RM and JZ created the concept of the project respecting ideas of UG and are responsible for funding acquisition. Methodology was developed by JZ and AR in close discussion with RM and UG. AR constructed the setup, conducted the investigation process and wrote the original draft. AR and ND developed supporting algorithms and computer code for equilibrium calculation, respectively. All authors contributed to the interpretation of the data and to the review and editing of the final paper. MM supervised the work and provided external mentorship.

https://doi.org/10.5194/jsss-9-355-2020

J. Sens. Sens. Syst., 9, 355–362, 2020

References

Crocoll, M. and Weisweiler, W.: Kinetische Untersuchungen zur Pt-katalysierten Oxidation von NO: Modellierung und Simulation, Chem. Ing.-Tech., 76, 1490–1494, https://doi.org/10.1002/cite.200403426, 2004.

Donker, N., Ruchets, A., Schönauer-Kamin, D., Zosel, J., Guth, U., and Moos, R.: Influence of polarization time and polarization current of Pt|YSZ-based NO sensors utilizing the pulsed polarization when applying constant charge, Sensor. Actuat. B-Chem., 290, 28–33, https://doi.org/10.1016/j.snb.2019.03.060, 2019.

Fischer, S., Pohle, R., Magori, E., Fleischer, M., and Moos, R.: Detection of NO by pulsed polarization of Pt I YSZ, Solid State Ionics, 262, 288–291, https://doi.org/10.1016/j.ssi.2014.01.022, 2014.

Jaccoud, A., Falgairette, C., Fóti, G., and Comninellis, C.: Charge storage in the $O_{2(g)}$,Pt/YSZ system, Electrochim. Acta, 52, 7927–7935, https://doi.org/10.1016/j.electacta.2007.06.046, 2007.

Miura, N., Raisen, T., Lu, G., and Yamazoe, N.: Highly selective CO sensor using stabilized zirconia and a couple of oxide electrodes, Sensor. Actuat. B-Chem., 47, 84–91, https://doi.org/10.1016/S0925-4005(98)00053-7, 1998.

Möbius, H.-H.: Solid-State Electrochemical Potentiometric Sensors for Gas Analysis, Sensors: Chemical and Biochemical Sensors – Part II, 3, 1105–1154, https://doi.org/10.1002/9783527620142.ch12, 1991.

Park, J.-H. and Blumenthal, R. N.: Electronic Transport in 8 Mole Percent Y_2O_3-ZrO_2, J. Electrochem. Soc., 136, 2867–2876, 1989.

Randles, J. E. B.: A cathode ray polarograph. Part II – The current-voltage curves, T. Faraday Soc., 44, 327–338, https://doi.org/10.1039/TF9484400327, 1948.

Ritter, T., Lattus, J., Hagen, G., and Moos, R.: Effect of the Heterogeneous Catalytic Activity of Electrodes for Mixed Potential Sensors, J. Electrochem. Soc., 165, B795–B803, https://doi.org/10.1149/2.0181816jes, 2018.

Ruchets, A., Donker, N., Schönauer-Kamin, D., Moos, R., Zosel, J., Guth, U., and Mertig, M.: Selectivity improvement towards hydrogen and oxygen of solid electrolyte sensors by dynamic electrochemical methods, Sensor. Actuat. B-Chem., 290, 53–58, https://doi.org/10.1016/j.snb.2019.03.063, 2019.

Schelter, M.: Entwicklung eines Festelektrolytsensor-Messsystems für die coulometrische Spurenanalytik, Technische Universität Dresden, Dresden, Thesis, 2015.

Schelter, M., Zosel, J., Oelßner, W., Guth, U., and Mertig, M.: A solid electrolyte sensor for trace gas analysis, Sensor. Actuat. B-Chem., 187, 209–214, https://doi.org/10.1016/j.snb.2012.10.111, 2013.

Schelter, M., Zosel, J., Oelßner, W., Guth, U., and Mertig, M.: Highly selective solid electrolyte sensor for the analysis of gaseous mixtures, J. Sens. Sens. Syst., 5, 319–324, https://doi.org/10.5194/jsss-5-319-2016, 2016.

Ševčík, A.: Oscillographic polarography with periodical triangular voltage, Collect. Czech. Chem. C., 13, 349–377, https://doi.org/10.1135/cccc19480349, 1948.

Shoemaker, E.: Cyclic voltammetry applied to an oxygen-ion-conducting solid electrolyte as an active electrocatalytic gas sensor, Solid State Ionics, 92, 285–292, https://doi.org/10.1016/S0167-2738(96)00419-5, 1996.

Teske, K., Popp, P., and Baumbach, J.: Solid-state coulometric cell as detector for gas chromatography, J. Chromatogr. A, 360, 417–420, https://doi.org/10.1016/S0021-9673(00)91690-X, 1986.

Yi, J., Kaloyannis, A., and Vayenas, C. G.: High temperature cyclic voltammetry of Pt catalyst-electrodes in solid electrolyte cells, Electrochim. Acta, 38, 2533–2539, https://doi.org/10.1016/0013-4686(93)80149-T, 1993.

Zhang, X., Kohler, H., Schwotzer, M., Wu, Y. H., and Guth, U.: Mixed-potential gas sensor with layered Au,Pt-YSZ electrode: Investigating the sensing mechanism with steady state and dynamic electrochemical methods, Sensor. Actuat. B-Chem., 252, 554–560, https://doi.org/10.1016/j.snb.2017.05.168, 2017.